Journal of Power Sources 196 (2011) 3781–3789

Contents lists available at ScienceDirect

Journal of Power Sources

journal homepage: www.elsevier.com/locate/jpowsour

Transient behavior analysis of a new designed passive direct methanol fuel cell fed with highly concentrated methanol

Weiwei Cai[a,c], Songtao Li[d], Ligang Feng[a,c], Jing Zhang[a,c], Datong Song[e], Wei Xing[a,*], Changpeng Liu[b,*]

[a] State Key Laboratory of Electroanalytical Chemistry, 5625 Renmin Street, Changchun, 130022, PR China
[b] Laboratory of Advanced Power Sources, Changchun Institute of Applied Chemistry, 5625 Renmin Street, Changchun, 130022, PR China
[c] Graduate School of the Chinese Academy of Sciences, 5625 Renmin Street, Changchun, 130022, PR China
[d] Institute of Mathematics, Jilin University, Changchun 130012, PR China
[e] Institute for Fuel Cell Innovation, National Research Council Canada, Vancouver, BC, Canada V6T 1W5

ARTICLE INFO

Article history:
Received 9 November 2010
Received in revised form
20 December 2010
Accepted 21 December 2010
Available online 7 January 2011

Keywords:
Passive direct methanol fuel cell
Highly concentrated methanol
Mathematical model

ABSTRACT

A new structure of passive direct methanol fuel cell (DMFC) with two methanol reservoirs separated by a porous medium layer is designed and a corresponding mathematical model is presented. The new designed passive DMFC can be directly fed with highly concentrated methanol solution or neat methanol. The porosity (ε_{pr}) of the porous medium layer is optimized using the proposed model. Some operation parameters are also optimized by both the numerical calculation and experimental measurement. The new designed DMFC can be continuously operated for about 4.5 times longer than a conventional passive DMFC with the optimum parameters. The methanol crossover during the same discharging is only about 50% higher.

1. Introduction

Direct methanol fuel cells (DMFCs) have attracted worldwide attention due to their high energy density and low-pollution [1]. There are two distinctions for fuel delivery system for DMFCs: active and passive. In the active DMFC, both methanol solution and air were supplied to the catalyst layer through flow fields using a liquid syringe pump and compressed gas cylinder. Compared with the active DMFC systems, both cathode and anode flow fields were removed in the passive DMFC systems and a fuel reservoir was placed at anode, methanol was delivered from fuel reservoir to anode catalyst layer by diffusion. Therefore, the passive DMFCs are considered as the most promising fuel cells for the portable electronic devices because of their simple structure [2]. However, there are a number of issues have to be solved before the commercialization of DMFCs, particularly the methanol crossover through the proton exchange membrane (PEM) [3]. Plenty of works have been carried out to reduce methanol crossover [4–10].

DMFC fed with dilute methanol solution is a facile way to alleviate the problem of methanol crossover (i.e., 1.0–2.0 mol L^{-1} for active methanol supply systems and 3.0–5.0 mol L^{-1} for passive methanol supply systems) [11–15]. However, using diluted methanol solution as the fuel for passive DMFCs will result in a short operation time as well as a low specific energy density because of the constant volume of the fuel reservoir. Hence it is urgent to find an effective fuel feeding strategy which is suitable for highly concentrated methanol feeding for the passive DMFCs. Many strategies have been developed to increase the transfer resistance of methanol from the fuel reservoir to anode catalyst layer (CL) in a passive DMFC to meet the objective of high concentration methanol feeding [16–20]. Abdelkareem et al. [16–18] added a dense porous carbon plate between fuel reservoir and anode CL of a passive DMFC. The data showed that the increased mass-transfer resistance of methanol resulting from the porous carbon plate makes it possible to feed high concentration methanol for the passive DMFC. When employing a 16.0 mol L^{-1} methanol solution, a maximum output power density of 24 mW cm^{-2} can be yielded at room temperature. In contrast to the conventional passive DMFCs, the current density decreased much more slowly during the 5.0 h discharging time under 0.1 V cell voltage. Kim et al. [19,20] added hydrogels into the fuel reservoir to reduce methanol diffusion from fuel reservoir to anode CL, so that the air-breathing passive DMFC can be operated at a high methanol concentration up to 8.0 mol L^{-1}. When the methanol concentration was changed from 4.0 mol L^{-1} to 8.0 mol L^{-1}, the maximum power density of the passive DMFC equipped with hydrogel fuel reservoir was increased from 16.5 mW cm^{-2} to 21.5 mW cm^{-2}, while the maximum power density of a conventional DMFC decreased from 14.0 mW cm^{-2} to

* Corresponding authors. Tel.: +86 431 85262223; fax: +86 431 85685653.
E-mail addresses: xingwei@ciac.jl.cn (W. Xing), liuchp@ciac.jl.cn (C. Liu).

0378-7753/$ – see front matter © 2011 Elsevier B.V. All rights reserved.
doi:10.1016/j.jpowsour.2010.12.083

Nomenclature

c_0^{MEOH}	methanol concentrations in DMR
c_{ac}^{MEOH}	methanol concentration in anode catalyst layer
c_{ad}^{MEOH}	local methanol concentration in anode diffusion layer
$c_{cc}^{O_2}$	oxygen concentration in cathode catalyst layer
$c_{cd}^{O_2}$	local oxygen concentration in cathode catalyst layer
c_h^{MEOH}	methanol concentrations in HMR
c_{pr}^{MEOH}	local methanol concentration in porous medium layer
c_{ref}^{MEOH}	reference methanol concentration
$c_{ref}^{O_2}$	reference oxygen concentration
D_{ad}^{MEOH}	diffusion coefficient of methanol in anode gas diffusion layer
$D_{cd}^{O_2}$	diffusion coefficient of oxygen in cathode gas diffusion layer
$D_{H_2O}^{MEOH}$	diffusion coefficient of methanol in water
D_m^{MEOH}	diffusion coefficient of methanol in PEM
D_{pr}^{MEOH}	diffusion coefficient of methanol in porous medium layer
E_{cell}^0	ideal electromotive force under standard condition
F	Faraday's constant
J	current density of the fuel cell
J_a	current density in anode side
J_{ct}	total current density in cathode side
j_{ref}^{MEOH}	reference exchange current density of anode
$j_{ref}^{O_2}$	reference exchange current density of cathode
l_0	thickness of reservoir for low concentration methanol
l_h	thickness of reservoir for high concentration methanol
N_{ad}	methanol flux through the anode diffusion layer
N_{cd}	oxygen flux through the cathode diffusion layer
N_m	methanol crossover flux through PEM
N_{pr}	methanol flux through PML
$n_d^{H_2O}$	electro-osmotic drag coefficient of water
n_d^{MEOH}	electro-osmotic drag coefficient of methanol
R	universal gas constant
R_{con}	contact resistance of cell
T	cell temperature

Greeks letters

α_a	anodic transfer coefficient
α_c	cathodic transfer coefficient
γ_a	order of anode reaction
γ_c	order of cathode reaction
δ_{pr}	thickness of porous layer
δ_m	thickness of membrane
δ_{ac}	thickness of anode catalyst layer
δ_{cc}	thickness of cathode catalyst layer
δ_{ad}	thickness of anode diffusion layer
δ_{cd}	thickness of cathode diffusion layer
σ_m	conductivity of PEM
ε	correction factor of diffusion coefficient
ε_{pr}	porosity of the PML
ε_{pr}^{eff}	effective porosity of porous medium layer
η_a	anodic overpotential
η_c	cathodic overpotential

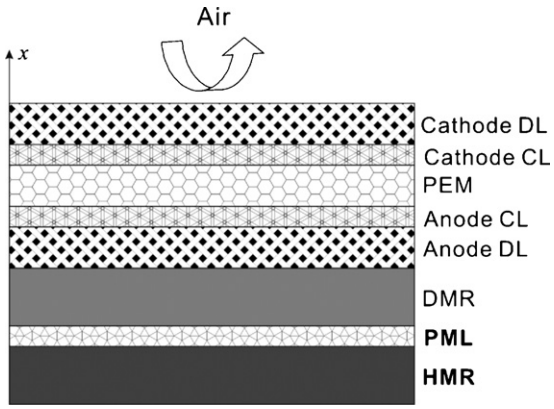

Fig. 1. Schematic diagram of the new designed passive DMFC with two fuel reservoirs. (DMR: diluted methanol reservoir; PML: porous medium layer; HMR: high concentration methanol reservoir).

a value smaller than 5.0 mW cm^{-2}. A semi-passive DMFC using porous PTFE plate as the methanol barrier layer (MBL) was manufactured by Li et al. [21,22]. A maximum output power density of 115.8 mW cm^{-2} can be obtained when MBL of 6.4 mm and Nafion 212 were used with 20 mol L^{-1} methanol supplied.

Above, all the previously reported designs can be operated with relative high concentration methanol solution. However, the employment of methanol-transfer-control layer will bring a much larger CO_2 releasing resistance than conventional passive DMFC, because CO_2 must transported through the same components as methanol in the above-mentioned designs. In order to realize the passive DMFC supplied with high methanol concentration, a passive DMFC with two methanol reservoirs separated by a porous medium layer (PML) is designed in the present paper as shown in Fig. 1. The methanol crossover can be well controlled in this DMFC, because the methanol concentration in anode catalyst layer can be controlled at a low level during the whole discharging process. Moreover, CO_2 transport in this DMFC does not pass through the PML, so that CO_2 releasing resistance in this new designed DMFC can keep the same as in the conventional DMFC. The continuous operation performance of this new DMFC is investigated by both mathematical model and experiments. Compared with the conventional DMFCs, the new designed DMFC can get much better continuous operation performance. The structural and operation parameters are also optimized by the mathematical model in this study.

2. Experimental

PtRu/C (60 wt.% Pt, Pt:Ru = 1:1) powder and Pt/C (60 wt.% Pt) powder were suspended respectively in 10% PTFE solution in an ultrasonic bath until a homogeneous ink was formed. After spraying the catalyst ink to 20% PTFE wet-proofed two 2 cm × 2 cm carbon papers, it was then cured at 340 °C in a nitrogen-filled vacuum oven for 1 h to form the anodic and cathode electrodes. The loadings of noble metal and Nafion® in both catalyst layers were about 4 mg cm^{-2}. The electrodes were hot pressed to the membrane at 130 °C and 5 MPa for 3 min to get a MEA.

Polycarbonate was chosen as the reservoir material, and 316L stainless steel palates with gold layer electroplated on the surface were used as current collectors. The conventional passive DMFC was fabricated following Ref. [23], the dimensions of the reservoir were 2 cm × 2 cm × 1 cm (thick). The new designed DMFC has two fuel reservoirs with the dimensions of 2 cm × 2 cm × 0.18 cm (thick) and 2 cm × 2 cm × 0.72 cm (thick) as shown in Fig. 1, and these two reservoirs were separated by porous medium layer (0.1 cm thick PTFE porous membrane).

After the MEA installed in the cell, methanol solution was directly fed into the fuel reservoirs. Both the polarization curves and discharging curves were measured at 25 °C.

3. Model description

3.1. Assumptions

The schematic diagram of the new designed passive DMFC is shown in Fig. 1, and this DMFC is named as H-DMFC because it can be fed with highly concentrated methanol solution.

The assumptions adopted for the model in this study are as follows:

1) The operation temperature of the DMFC is assumed to be uniform and the electrochemical reaction occurs at a constant temperature of 25 °C.
2) The concentration gradient of the reactants across the catalyst layers is ignored because the thickness of the catalyst layer is much smaller than that of the diffusion layer.
3) The methanol which permeates from anode CL to cathode CL is assumed to be completely consumed by the electrooxidation reaction [24] at the boundary between PEM and cathode CL, where consequently the methanol concentration drops to zero.
4) Methanol concentrations in the high concentration methanol reservoir (HMR) and the diluted methanol reservoir (DMR) are assumed to be uniform, respectively. The H-DMFC discussed in this work has a constant HMR/DMR volume ratio of 4:1.

3.2. Mass transfer equations

Methanol permeation flux through PML, which is the methanol-transfer-control layer in H-DMFC, can be described by Fick's law

$$N_{pr} = -D_{pr}^{MEOH} \frac{\partial c_{pr}^{MEOH}}{\partial x} \quad (1)$$

where N_{pr} is the methanol flux, c_{pr}^{MEOH} is the methanol concentration, x is the coordinate, and D_{pr}^{MEOH} is the effective diffusion coefficient of methanol in the PML and can be estimated by Bruggeman's relation [25] as,

$$D_{pr}^{MEOH} = \varepsilon_{pr}^{1.5} D_{H_2O}^{MEOH} \quad (2)$$

where ε_{pr} is the porosity of the PML and $D_{H_2O}^{MEOH}$ is the diffusivity of methanol in liquid water.

Methanol flux across the anode diffusion layer N_{ad} is calculated by the following equation

$$N_{ad} = -D_{ad}^{MEOH} \frac{\partial c_{ad}^{MEOH}}{\partial x} \quad (3)$$

where c_{ad}^{MEOH} is the methanol concentration, and D_{ad}^{MEOH} is the effective diffusivity of methanol in anode diffusion layer.

The methanol crossover through the PEM is caused by both methanol diffusion and electro-osmotic drag, and can be estimated as

$$N_m = -D_m^{MEOH} \frac{\partial c_m^{MEOH}}{\partial x} + n_d^{MEOH} \frac{J}{F} \quad (4)$$

where c_m^{MEOH} is the methanol concentration, D_m^{MEOH} is the effective diffusion coefficient of methanol in PEM, N_m is the methanol crossover flux, n_d^{MEOH} is the electro-osmotic drag, J is operation current density of the DMFC, F is Faraday's constant. First term on the right-hand side of Eq. (4) represents the methanol diffusion across the PEM, and the second term describes the methanol permeation through the PEM caused by the electro-osmotic drag.

In the cathode diffusion layer, oxygen flux can be also expressed by Fick's law because of no external convection exists in the cathode side of an passive DMFC, so

$$N_{cd} = D_{cd}^{O_2} \frac{\partial c_{cd}^{O_2}}{\partial x} \quad (5)$$

where N_{cd} is the methanol flux, $c_{cd}^{O_2}$ is the oxygen molar concentration, and $D_{cd}^{O_2}$ is the effective diffusivity of oxygen in cathode diffusion layer.

3.3. Conservation equations

The methanol flux through the anode diffusion layer is consumed through two routes: methanol electrooxidation in anode catalyst layer and methanol permeation across the PEM. The electrochemical reaction in anode CL of DMFC is

$$CH_3OH + H_2O \rightarrow CO_2 + 6H^+ + 6e^- \quad (6)$$

According to this reaction formula, 1 mol methanol can produce 6 mol protons and 6 mol electrons. Thus

$$N_{ad} = \frac{1}{6F} J + N_m \quad (7)$$

In the cathode CL of DMFC, two reactions are proceeding simultaneously. The expected reaction is the oxygen electroreduction, every 1.5 mol O_2 reacts with 6 mol protons and 6 mol electrons through the following equation:

$$1.5O_2 + 6H^+ + 6e^- \rightarrow 3H_2O \quad (8)$$

The other reaction occurs in cathode CL is the consumption of permeated methanol from anode side,

$$\begin{cases} CH_3OH + H_2O \rightarrow CO_2 + 6H^+ + 6e^- \\ 1.5O_2 + 6H^+ + 6e^- \rightarrow 3H_2O \end{cases} \quad (9)$$

Therefore, the oxygen flux across the cathode gas diffusion layer can be determined by the conservation equation:

$$N_{cd} = \frac{1}{4F} J + \frac{3}{2} N_m \quad (10)$$

3.4. Potential equations

Butler–Volmer expression is used to describe the relationship between current density and overpotential in both anode and cathode catalyst layers

$$J_a = J_{ref}^{MEOH} \left(\frac{c_{ac}^{MEOH}}{c_{ref}^{MEOH}} \right)^{\gamma_a} \exp\left(\frac{\alpha_a F}{RT} \eta_a \right) \quad (11)$$

$$J_{ct} = J_{ref}^{O_2} \left(\frac{c_{cc}^{O_2}}{c_{ref}^{O_2}} \right)^{\gamma_c} \exp\left(\frac{\alpha_c F}{RT} \eta_c \right) \quad (12)$$

where η_a and η_c are overpotentials in anode and cathode side, respectively. J_a is the current density in anode side and $J_a = J$, while J_{ct} is defined as the total current density in cathode side. The permeated methanol is considered to be consumed by electrooxidation reaction in the cathode catalyst layer, so

$$J_{ct} = J + 6FN_m \quad (13)$$

Table 1
Parameter values.

Parameter/symbol (unit)	Value	Ref.
Cell temperature/T (K)	298.15	
Reference methanol concentration/c_{ref}^{MEOH} (mol cm^{-3})	1×10^{-3}	[26]
Reference oxygen concentration/$c_{ref}^{O_2}$ (mol cm^{-3})	$1\times10^{-6}\times101325/(RT)$	[26]
Diffusion coefficient of methanol in anode gas diffusion layer/D_{ad}^{MEOH} (cm^2 s^{-1})	$\varepsilon D_{H_2O}^{MEOH}$	[26]
Diffusion coefficient of methanol in water/$D_{H_2O}^{MEOH}$ (cm^2 s^{-1})	$2.8\times10^{-6}\exp(2436/353)-(2436/T))$	[26]
Correction factor of diffusion coefficient/ε	0.55	[27]
Diffusion coefficient of methanol in membrane/D_m^{MEOH} (cm^2 s^{-1})	$4.9\times10^{-6}\exp(2436/333)-(2436/T)$	[26]
Ideal electromotive force under standard condition/E_{cell}^0 (V)	1.213	[28]
Faraday's constant/F	96,487	
Reference exchange current density of anode/j_{ref}^{MEOH} (A cm^{-2})	$0.011\times\delta_{ac}$	[29]
Thickness of cathode catalyst layer/δ_{ac} (cm)	0.005	Assumed
Reference exchange current density of cathode/$j_{ref}^{O_2}$ (A cm^{-2})	$0.011\times\delta_{cc}$	[29]
Thickness of cathode catalyst layer/δ_{cc} (cm)	0.005	Assumed
Thickness of reservoir for low concentration methanol/l_0 (cm)	0.18	
Thickness of reservoir for high concentration methanol/l_h (cm)	0.72	
Electro-osmotic drag coefficient of methanol/n_d^{MEOH}	$x^{MEOH}n_d^{H_2O}$	[30]
Electro-osmotic drag coefficient of water/$n_d^{H_2O}$	$2.9\exp(1029/333)(1029/T)$	[27]
Contact resistance of cell/R_{con} (Ω cm^2)	0.8	Assumed
Conductivity of PEM/σ_m (S cm^{-1})	$0.073\exp(1268((1/298)-(1/T)))$	[26]
Order of anode reaction/γ_a	1	Assumed
Order of cathode reaction/γ_c	1	Assumed
Anodic transfer coefficient/α_a	0.5	Assumed
Cathodic transfer coefficient/α_c	0.5	Assumed
Thickness of porous layer/δ_{pr} (cm)	0.1	
Thickness of membrane/δ_m (cm)	0.015	
Thickness of anode diffusion layer/δ_{ad} (cm)	0.003	
Thickness of cathode diffusion layer/δ_{cd} (cm)	0.003	

3.5. Numerical analysis

According to assumptions 3 and 4 in Section 3.1, Eqs. (1)–(4) can be rewritten as follows

$$\begin{cases} N_{pr} = D_{pr}^{MEOH}\dfrac{c_h^{MEOH}-c_0^{MEOH}}{\delta_{pr}} \\ N_{ad} = D_{ad}^{MEOH}\dfrac{c_0^{MEOH}-c_{ac}^{MEOH}}{\delta_{ad}} \\ N_m = D_m^{MEOH}\dfrac{c_{ac}^{MEOH}}{\delta_m} + n_d^{MEOH}\dfrac{J_a}{F} \\ N_{cd} = \dfrac{D_{cd}^{O_2}}{\delta_{cd}}(c_{amb}^{O_2}-c_{cc}^{O_2}) \end{cases} \quad (14)$$

c_h^{MEOH} and c_0^{MEOH} here represent the methanol concentrations in HMR and DMR, respectively, and $c_{amb}^{O_2}$ is the oxygen concentration in the ambient air. δ_{pr}, δ_{ad} δ_m and δ_{cd} are the thicknesses of the corresponding layers, respectively.

The methanol consumption only happens in the anode and cathode catalyst layer. Therefore, when the fuel cell is working under a constant current density, values of c_h^{MEOH} and c_0^{MEOH} during the discharge process can be calculated by the following differential equations:

$$\begin{cases} \dfrac{\partial c_h^{MEOH}}{\partial t} = -\dfrac{N_{pr}}{l_h} \\ \dfrac{\partial c_0^{MEOH}}{\partial t} = \dfrac{N_{pr}-N_{ad}}{l_0} \end{cases} \quad (15)$$

The initial conditions for Eq. (15): $c_h^{t=0}=c_h^{int}$ and $c_0^{t=0}=c_0^{int}$. Combining with Eq. (14), the solutions for c_h^{MEOH} and c_0^{MEOH} can be easily obtained.

The cell voltage is determined by the following equation

$$V = E_{cell}-\eta_a-\eta_c-JR_{con}-J\frac{\delta_m}{\sigma_m} \quad (16)$$

where E_{cell} is the electromotive force, which can be calculated by $E_{cell}=E_{cell}^0+(T-T_0)(\partial E_{cell}/\partial T)$, and E_{cell}^0 is the electromotive force under standard conditions.

4. Results and discussion

The conventional DMFC investigated in this work has a fuel reservoir with a thickness of 1.0 cm, while the thickness of DMR and HMR in H-DMFC is 0.18 cm and 0.72 cm, respectively. The cross-sectional area of the reservoirs is equivalent with the active area of the electrode.

4.1. Estimation of model parameters

Most of the parameters in the analytical solution could be found in the literatures as given in Table 1, but some need to be assumed to fit the experimental results. Therefore, the comparison of the experimental polarization data and modeling results for a conventional air-breathing passive DMFC is illustrated in Fig. 2a to estimate the assumed parameters. Three different concentrations are fed for the DMFC. The calculated results agree well with the experimental data except at the region of activation polarization.

The model parameters are also estimated by the transient cell voltage test under constant current density of both conventional DMFC and H-DMFC. A 0.1 cm thick porous medium layer (PML) is used for the H-DMFC, and the porosity of this PML is 0.4. The DMR and HMR are fed with 2.0 mol L^{-1} methanol solution and neat methanol, respectively. The conventional DMFC is fed with 3.0 mol L^{-1} methanol solution. The operation current density for both the H-DMFC and conventional DMFC is 60 mA cm^{-2}. It is shown in Fig. 2b that the experimental and calculated results have good agreements for these two DMFCs. However, the experimental continuous operation time is about 2.0 h shorter than the calculated one for H-DMFC. This difference is caused by the methanol evaporation, which is not taken into account in the mathematical model, during the discharging process. One can also conclude that the H-DMFC has a much better discharging performance than the conventional DMFC from Fig. 2b.

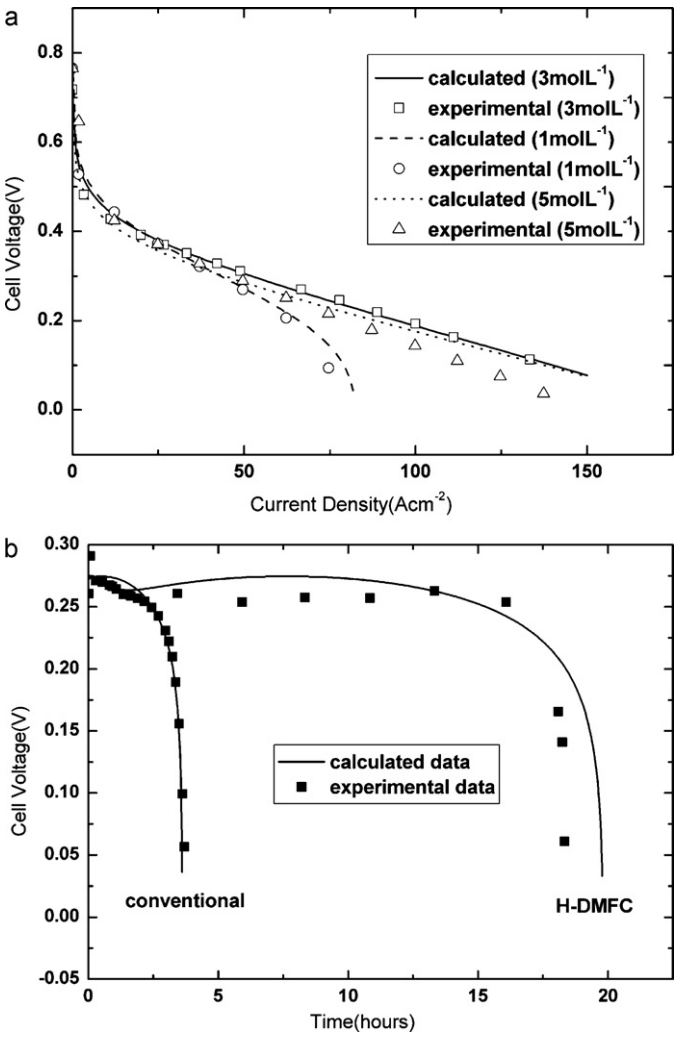

Fig. 2. Experimental and calculated (a) polarization data for a conventional DMFC; (b) transient cell voltage data for a conventional DMFC and a H-DMFC.

The rest part of this section will focus on the transient behavior analysis and parametric study of H-DMFC. The dependence of the H-DMFC's performance on porosity of PML is investigated in details, while the thickness of the PML is maintained at 0.1 cm. Meanwhile, the operation parameters, such as operation current density, methanol concentration are also discussed.

4.2. Effect of PML porosity

Porous medium layers with various porosities are invited in the model to investigate the continuous operation performance and to further optimize the porosity of porous medium layer. Fig. 3 gives the discharging curves of H-DMFCs with PML porosities ranging from 0.1 to 0.7 at 60 mA cm^{-2}. The methanol solutions fed in HMR and DMR are 20.0 mol L^{-1} and 3.0 mol L^{-1}, respectively. The discharging time increases rapidly with the increasing of the PML porosity (ε_{pr}), and gets a maximum value at the porosity 0.4. When ε_{pr} is 0.1, the H-DMFC can be continuously operated for only about 1.0 h, which is even much shorter than the discharging time of the conventional DMFC. The reason is that the methanol supplement from HMR to DMR cannot satisfy the methanol consumption by electrochemical reaction in anode CL. When ε_{pr} comes to 0.4, the continuous operation time increases to about 17 h, which is more than 3 times longer than that of the conventional DMFC. Further increasing the MPL porosity will gradually decrease the discharging time.

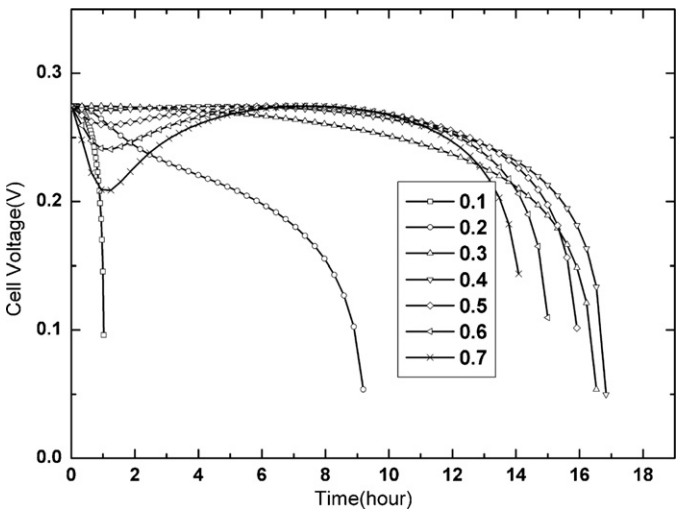

Fig. 3. Calculated discharging curves of the H-DMFC with different PML porosities ranging from 0.1 to 0.7 at 60 mA cm^{-2}.

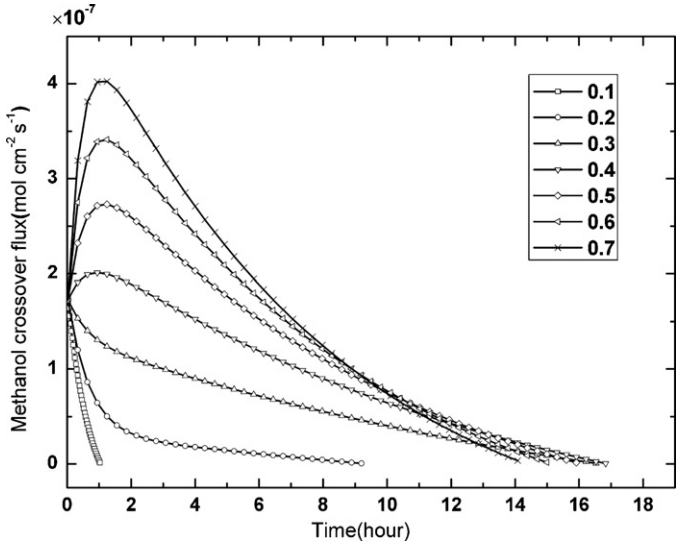

Fig. 4. Methanol crossover fluxes of the H-DMFC during the discharging process with different MPL porosities.

Fig. 4 compares the variation of the methanol crossover flux with time at different MPL porosities during the discharging process. When ε_{pr} is 0.1, methanol crossover flux falls rapidly with time because of the low methanol permeation velocity through MPL. Methanol crossover flux decreases with time but increases with MPL porosity when ε_{pr} is smaller than 0.3. After ε_{pr} increases over 0.3, the methanol crossover flux increases during the first hour because of the quick increasing of methanol concentration in DMR. This increment is caused by the large methanol flux through MPL compared with methanol crossover flux. The methanol crossover flux gets its climax at about 1.0 h and then decreases with time. When ε_{pr} is 0.7, the maximum value of the methanol crossover flux is larger than 4.0×10^{-7} mol cm^{-2} s^{-1}, which is about two times the quantity of the initial crossover flux value.

To optimize the porosity of PML, average power density during the discharging process is calculated and shown in Fig. 5. The case of $\varepsilon_{pr} = 0.1$ can be eliminated from the porosity optimization because of its ultra short discharging time. The average power density keeps growing with the increasing of ε_{pr} and has a maximum value when $\varepsilon_{pr} = 0.5$. And the discharging time reaches a maximum value at $\varepsilon_{pr} = 0.4$. In contrast with the case $\varepsilon_{pr} = 0.5$, the discharging

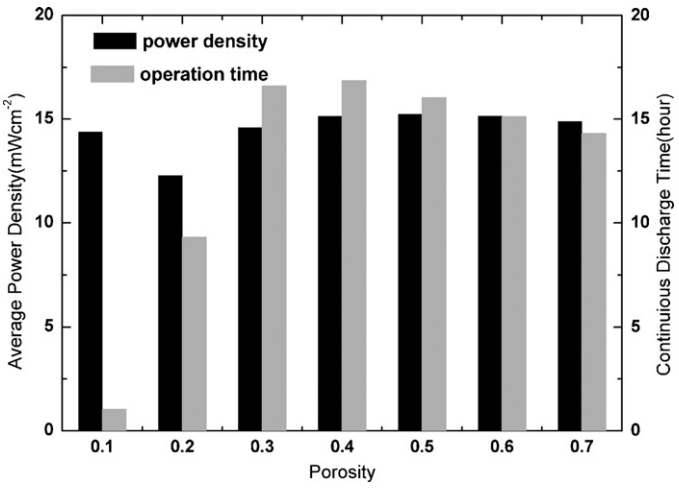

Fig. 5. Comparisons of average power density and continuous operation time of the H-DMFCs using different PML with porosities ranging from 0.1 to 0.7.

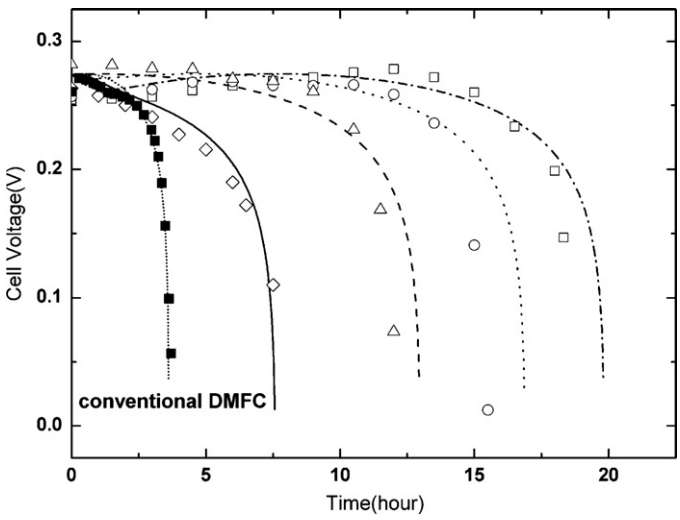

Fig. 6. Discharging curves of a conventional DMFC and H-DMFC with different methanol concentrations fed in the HMR at 60 mA m^{-2} (lines: solid—10 mol L^{-1} (calculated); dash—15 mol L^{-1} (calculated); dot—20 mol L^{-1}(calculated); dash dot—neat methanol (calculated); symbols: ◊—10 mol L^{-1} (experimental); △—15 mol L^{-1} (experimental); ○—20 mol L^{-1} (experimental); □—neat methanol (experimental)).

time in the case of ε_{pr} = 0.4 is 0.8 h longer, while the average power density is only 0.1 mW cm^{-2} smaller. Therefore 0.4 is considered as the optimum value for the PML porosity.

From the above discussions, one can conclude from the calculated results that the appropriate using of PML in the DMFC can improve the discharging time notably without deteriorating the output power density. Taking the two factors into account, we choose 0.4 as the optimum value for PML porosity.

4.3. Effect of operation parameters

Operation parameters studied in this work contain the methanol concentration fed in HMR and DMR and the operation current density. The optimized value of the PML's porosity is used in this section while the other structural parameters keep the same as in Section 4.2.

4.3.1. Methanol concentration fed in HMR

In Fig. 6, we investigate the effects of methanol concentration in HMR on the transient performance of H-DMFC by both experimental measurement and numerical calculation. The DMR is fed with 3.0 mol L^{-1} methanol solution and the operation current density is 60 mA cm^{-2}. Fuel fed in HMR varies from 10.0 mol L^{-1} methanol solution to neat methanol. The discharging curve of a conventional DMFC fed with 3.0 mol L^{-1} methanol solution is also shown in Fig. 6.

The experimental results agree well with the numerical predication as shown in Fig. 6. This result can further verify the proposed mathematical model. The discharging time increases significantly with methanol concentration in HMR. The continuous operation time of the H-DMFC has about 5.0 h increment for each 5.0 mol L^{-1} methanol concentration increasing and up to about 20.0 h when neat methanol is fed in HMR. This is about 4.5 times longer than the continuous operation time of the conventional DMFC fed with 3.0 mol L^{-1} methanol solution.

Meanwhile, the variations of methanol crossover fluxes are shown in Fig. 7, and the average crossover fluxes are given in the inset. We can see that the average methanol crossover fluxes in the neat methanol case is about 200% higher than the flux in the 10.0 mol L^{-1} case, while it is only about 50% higher than that of a conventional DMFC.

Fig. 8a is the bar diagram of calculated average power density and continuous operation time of the H-DMFC with different methanol concentrations fed in HMR. Although the methanol crossover increases visibly with the methanol concentration in HMR, the average power density of the H-DMFC does not deteriorate with the increasing of methanol concentration because of the decreased anodic overpotential as shown in Fig. 8b. It can be seen from Fig. 8a that the average power density even slightly increases with the methanol concentration. Therefore, we can conclude that neat methanol is the optimum fuel for HMR, because of the longest discharging time as well as the highest average power density can be obtained in this case.

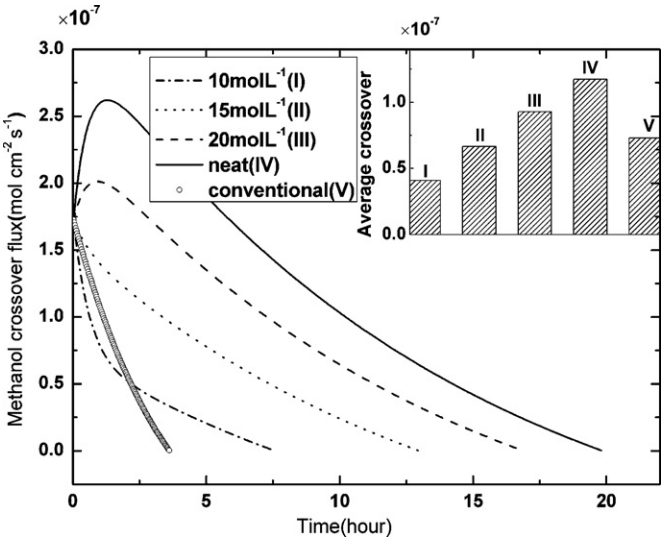

Fig. 7. Evolution of methanol crossover flux for a conventional DMFC and H-DMFC with different methanol concentrations fed in the HMR at 60 mA cm^{-2}.

4.3.2. Methanol concentration fed in DMR

The calculated discharging curves at 60 mA cm^{-2} with different methanol concentrations fed in DMR and neat methanol fed in HMR are shown in Fig. 9a. The change of discharging time with the methanol concentration in DMR is neglectable and the five discharging curves are almost identical except the initial 3 h. The variations of cell voltage during the first 3 h are enlarged in Fig. 9b. When 1.0 mol L^{-1} methanol solution is fed in DMR, the H-DMFC has the lowest cell voltage at the initial stage among the five cases because of its highest anodic overpotential (η_a) as shown

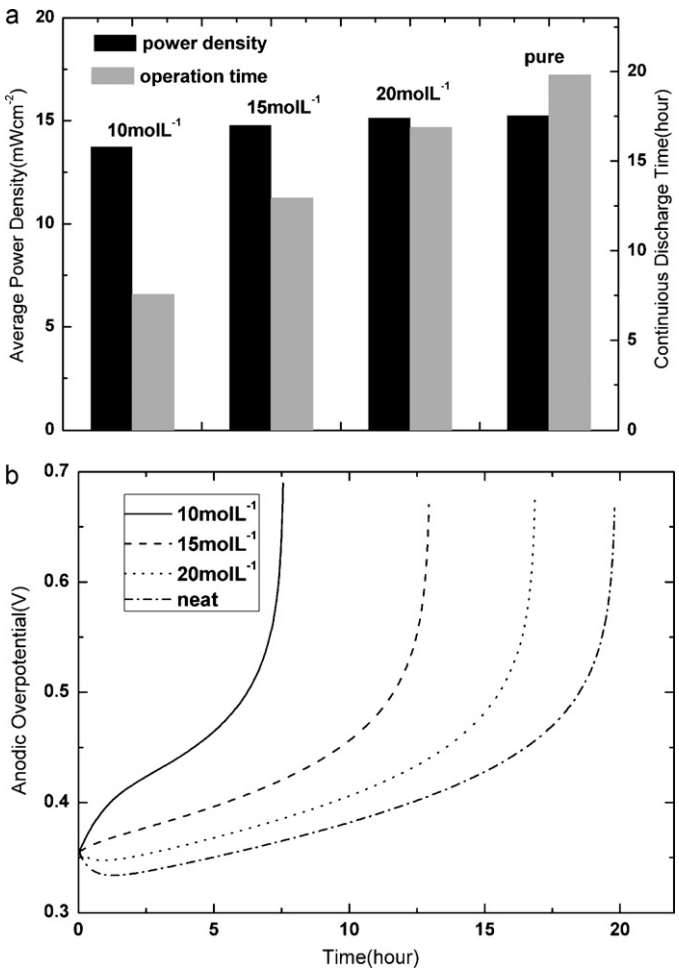

Fig. 8. (a) Bar diagrams of average power density and continuous operation time; (b) variation of anodic overpotential for the H-DMFC fed with different concentration methanol solution in HMR.

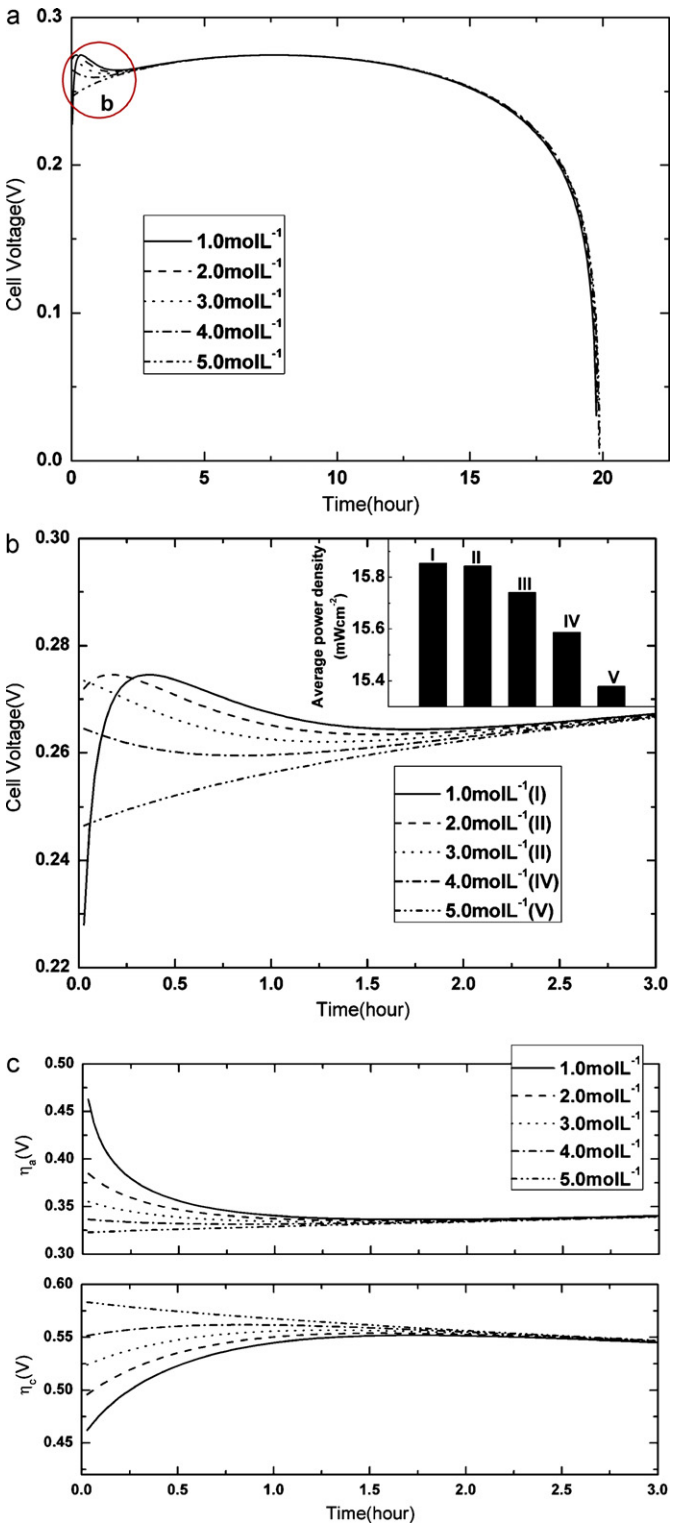

Fig. 9. (a, b) Evolutions of cell voltage of the H-DMFC; (c) anodic and cathodic overpotential with different methanol concentrations fed in DMR.

in Fig. 9c. After 0.5 h discharging, the cell voltage for 1.0 mol L^{-1} case increases swiftly and becomes the highest one, because the difference of η_a among the five cases becomes very small and the cathode overpotential (η_c) turns to be the determinant factor for the difference among cell voltages.

Overall, the difference among transient performances is neglectable when the methanol concentration in DMR is changing from 1.0 to 5.0 mol L^{-1}. But there is a great transient performance difference in terms of changing the concentration in HMR as discussed in Section 4.3.1. The reason is that changing the concentration in DMR will not affect the methanol concentrations either in DMR (c_0) or in anode catalyst layer (c_{ac}) notably during the discharging process as shown in Fig. 10. While c_{ac} is the determine factor for both anodic overpotential and methanol crossover.

The methanol crossover fluxes with different methanol concentrations in DMR are displayed in Fig. 11a and their average values are plotted in Fig. 11b. It can be seen from Fig. 11a that the five curves cannot be differentiated after 3.0 h and the average value of methanol crossover flux only has a difference about 10^{-8} mol cm^{-2} s^{-1} between1.0 mol L^{-1} and 5.0 mol L^{-1} cases, which is caused by the difference of methanol crossover fluxes in the first 3.0 h. Meanwhile, the comparison of average power densities during the discharge process is also shown in Fig. 11b. When DMR is fed with 2.0 mol L^{-1} methanol solution, the maximum average power density is obtained, which is about 0.08 mW cm^{-2} higher than that of the 5.0 mol L^{-1}. Therefore, 2.0 mol L^{-1} is chosen as the optimum methanol concentration fed in DMR, which is diluter than the commonly used ones (3.0–5.0 mol L^{-1}) in conventional DMFCs.

4.3.3. Operation current density

The methanol crossover flux of H-DMFC depends strongly on the operation current density, because both the methanol consumption by electrochemical reaction in anode CL and methanol perme-

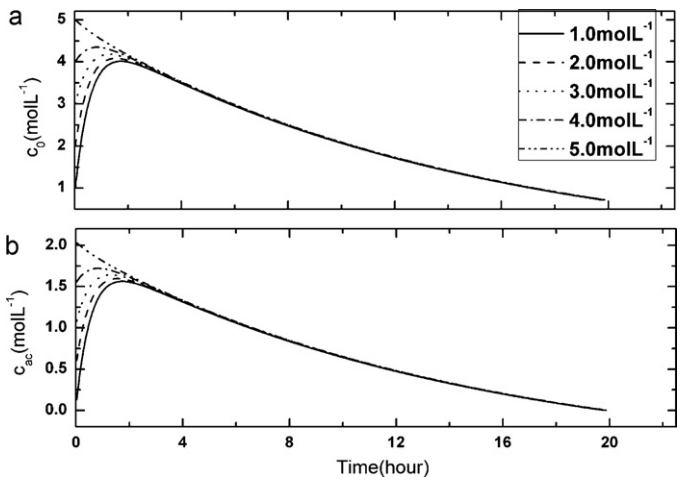

Fig. 10. Evolutions of methanol concentration in (a) DMR; (b) anode catalyst layer with different methanol concentrations fed in DMR.

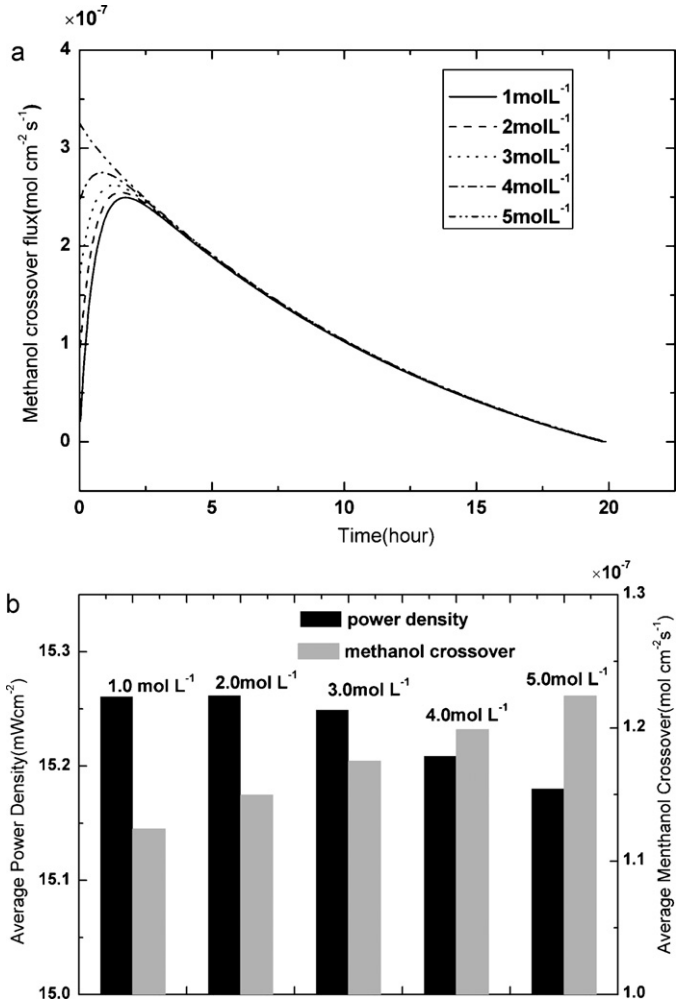

Fig. 11. (a) Variations of methanol crossover flux; (b) comparisons of the average power density and average crossover flux during the discharge process.

ation caused by electro-osmotic drag are determined by current density. So the changes of methanol crossover flux of H-DMFC at different current densities are calculated out and shown in Fig. 12. And the optimum PML porosity and the methanol concentrations in HMR and DMR are employed for this methanol crossover calculation. Compared with the 40 mA cm^{-2} case, the peak value of

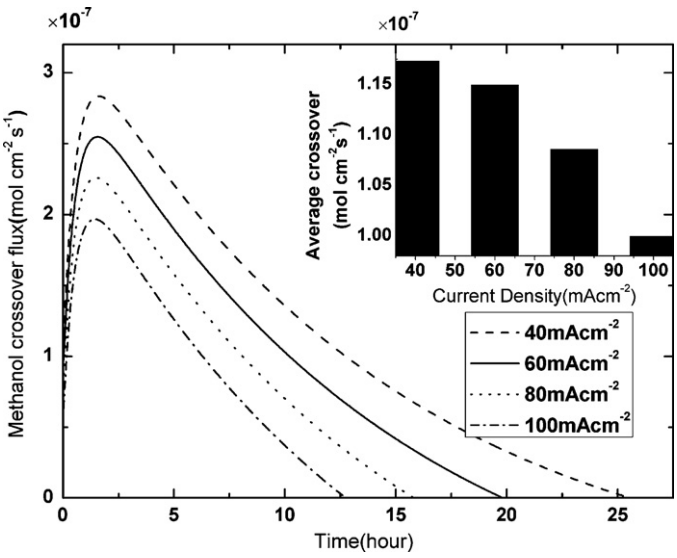

Fig. 12. Evolution of methanol crossover flux of the H-DMFC at different current densities.

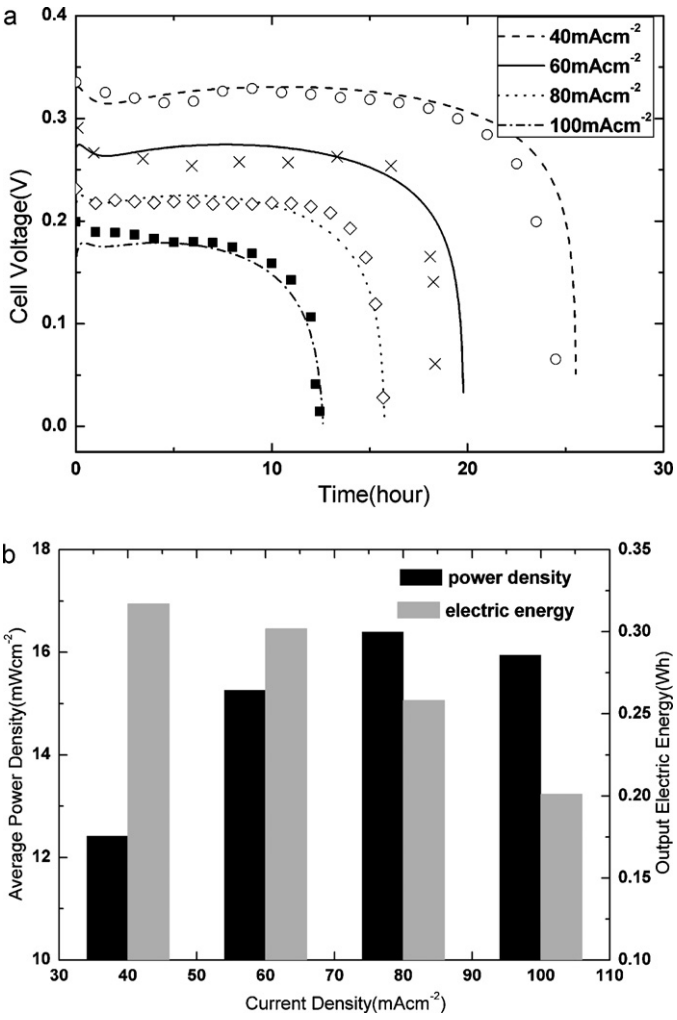

Fig. 13. (a) Evolution of cell voltage (b) average power density and total electric energy output of the H-DMFC at different operation current densities.

the methanol crossover flux for 100 mA cm^{-2} case is about 50% smaller, and the average crossover is 15% smaller. This difference of methanol crossover flux is caused by the lower methanol concentration in anode CL when higher current density is used.

The corresponding cell voltage variations obtained by both experimental measurement and numerical calculation are shown in Fig. 13a. The calculated curves show very good agreements with the experimental data for all the four current densities. It can be found that the higher operation current density is used, the shorter discharging time and lower cell voltage can be obtained. In the case of 40 mA cm^{-2}, the cell voltage of H-DMFC can maintain above 0.3 V for more than 20 h, and stop at about 25 h. When the operation current density increases to 100 mA cm^{-2}, the H-DMFC can continuously be operated for more than 10 h with the cell voltage above 0.15 V. The average power densities and electric energy outputs per square centimeter at different current densities are calculated and displayed in Fig. 13b. As seen from the figure, the smaller current density is used, the higher electric energy output can be obtained. This high electric energy means a high utilization rate of fuel. The reason is that the higher current density is used, the more energy is lost as waste heat. The average power density has a maximum value of 16.4 mW cm^{-2} at 80 mA cm^{-2}, while the electric energy output keeps decreasing with increasing operation current density. The decrease of electric energy output is primarily caused by the difference of the continuous operation time for these cases.

Taking discharge performance into account, it is found that the H-DMFC with optimized structural and operation parameters can obtain much longer discharging time than the conventional DMFC. And the highest power density can be obtained at about 80 mA cm^{-2}.

5. Conclusions

Porous medium layer is used as methanol-diffusion-control material in our new designed passive DMFC. The porous medium layer positioned between two separated fuel reservoirs makes it possible to feed high concentration methanol solution or neat methanol in the anode side of the DMFC directly. The advantage of the new design is verified by the transient performance compared with a conventional passive DMFC at the same conditions and the continuous operation time is 5.5 times the length of the continuous operation time of a conventional DMFC.

A numerical model is also developed and a parametric study is conducted to investigate the effects of structural and operation parameters on the transient performance of the new designed DMFC. It can be concluded as follows:

1) The best continuous transient performance can be obtained when the porous medium layer with a porosity of 0.4 is used in H-DMFC.
2) The transient performance of the H-DMFC depends on the methanol concentration in HMR intensely. While the effect of the methanol concentration in DMR on the performance of the H-DMFC is almost neglectable. Neat methanol and is considered to be the optimum fuel for HMR by the verification of both numerical calculation and experimental measurement.
3) Highest power density output of the H-DMFC can be obtained at the current density about 80 mA cm^{-2}.

Acknowledgments

This work was supported by National Natural Science Foundation of China (Nos. 20876153, 20703043, 21073180, 21011130027 and 20933004), Science & Technology Research Programs of Jilin Province (20102204), and National High Technology Research and Development Program of China (863 Program, Nos. 2007AA05Z159, 2007AA05Z143).

References

[1] R. Dillon, S. Srinivasan, A.S. Arico, V. Antonucci, J. Power Sources 127 (2004) 112–126.
[2] T.S. Zhao, R. Chen, W.W. Yang, C. Xu, J. Power Sources 191 (2009) 185–202.
[3] K.M. McGrath, G.K.S. Prakash, G.A. Olah, J. Ind. Eng. Chem. 10 (2004) 1063–1080.
[4] I. Chang, S. Ha, S. Kim, S. Kang, J. Kim, K. Choi, S.W. Cha, J. Power Sources 188 (2009) 205–212.
[5] P.X. Xing, G.P. Robertson, M.D. Guiver, S.D. Mikhailenko, K.P. Wang, S. Kaliaguine, J. Memb. Sci. 229 (2004) 95–106.
[6] S. Reichman, L. Burstein, E. Peled, J. Power Sources 179 (2008) 520–531.
[7] D. Yamamoto, H. Munakata, K. Kanamura, J. Electrochem. Soc. 155 (2008) B303–B308.
[8] J. Saito, K. Miyatake, M. Watanabe, Macromolecules 41 (2008) 2415–2420.
[9] S.N. Xue, G.P. Yin, Polymer 47 (2006) 5044–5049.
[10] H.W. Zhang, X.H. Fan, J. Zhang, Z.T. Zhou, Solid State Ionics 179 (2008) 1409–1412.
[11] M.K. Ravikumar, A.K. Shukla, J. Electrochem. Soc. 143 (1996) 2601–2606.
[12] S. Surampudi, S.R. Narayanan, E. Vamos, H. Frank, G. Halpert, A. Laconti, J. Kosek, G.K.S. Prakash, G.A. Olah, J. Power Sources 47 (1994) 377–385.
[13] R. Chen, T.S. Zhao, J. Power Sources 152 (2005) 122–130.
[14] B. Bae, B.K. Kho, T.H. Lim, I.H. Oh, S.A. Hong, H.Y. Ha, J. Power Sources 158 (2006) 1256–1261.
[15] J.G. Liu, T.S. Zhao, R. Chen, C.W. Wong, Electrochem. Commun. 7 (2005) 288–294.
[16] N. Nakagawa, M.A. Abdelkareem, K. Sekimoto, J. Power Sources 160 (2006) 105–115.
[17] M.A. Abdelkareem, N. Nakagawa, J. Power Sources 162 (2006) 114–123.
[18] M.A. Abdelkareem, N. Morohashi, N. Nakagawa, J. Power Sources 172 (2007) 659–665.
[19] W.J. Kim, H.G. Choi, Y.K. Lee, J.D. Nam, S.M. Cho, C.H. Chung, J. Power Sources 157 (2006) 193–195.
[20] W.J. Kim, H.G. Choi, Y.K. Lee, J.D. Nam, S.M. Cho, C.H. Chung, J. Power Sources 163 (2006) 98–102.
[21] X.L. Li, A. Faghri, C. Xu, Int. J. Hydrogen Energy 35 (2010) 8690–8698.
[22] X.L. Li, A. Faghri, C. Xu, J. Power Sources 195 (2010) 8202–8208.
[23] T. Shimizu, T. Momma, M. Mohamedi, T. Osaka, S. Sarangapani, J. Power Sources 137 (2004) 277–283.
[24] J.T. Wang, S. Wasmus, R.F. Savinell, J. Electrochem. Soc. 143 (1996) 1233–1239.
[25] R.E. Delarue, C.W. Tobias, J. Electrochem. Soc. 106 (1959) 827–833.
[26] K. Scott, W. Taama, J. Cruickshank, J. Power Sources 65 (1997) 159–171.
[27] H. Guo, C.F. Ma, Electrochem. Commun. 6 (2004) 306–312.
[28] O. Zerbinati, A. Mardan, M.M. Richter, J. Chem. Educ. 79 (2002) 829–831.
[29] A.A. Kulikovsky, Electrochem. Commun. 4 (2002) 939–946.
[30] Z.H. Wang, C.Y. Wang, J. Electrochem. Soc. 150 (2003) A508–A519.